Available online at www.sciencedirect.com
ScienceDirect
Journal of Organometallic Chemistry 692 (2007) 1039–1047
Journal of Organometallic Chemistry
www.elsevier.com/locate/jorganchem

Study of the structural and electronic properties of 1-(4, 5 and 6-selenenyl derivatives-3-formyl-phenyl) pyrrolidinofullerenes

Abraham F. Jalbout [a,*], Ali Jameel Hameed [b,*], Bartosz Trzaskowski [c]

[a] Institute of Chemistry, National Autonomous University of Mexico, Mexico City, Mexico
[b] Department of Chemistry, College of Science, University of Basrah, Basrah, Iraq
[c] NASA Astrobiology Institute, Department of Chemistry, University of Arizona, Tucson, AZ, USA

Received 17 August 2006; received in revised form 26 October 2006; accepted 26 October 2006
Available online 10 November 2006

Abstract

A series of 1-(4, 5 and 6-selenenyl derivatives-3-formyl-phenyl) pyrrolidinofullerenes molecules C_{60}–C_2H_4N–[3-(CHO)C_6H_3SeX] were investigated theoretically by performing Density Functional Theory calculations at the B3LYP/3-21G* level of the theory. The substituents include: X = CN, $CH_2CH(NH_2)CO_2H$ and $CH_2CH_2CH(NH_2)CO_2H$. We have selected these substituents to be in *ortho*, *meta* and *para* positions with relation to formyl group in order to show the effect of such structural change on the electronic properties of the molecules. The theoretical IR spectra, physical, chemical and thermodynamics properties of the molecules studied are obtained and discussed.

Keywords: Fullerene; Selenium; Organoselenium compounds; Fulleropyrrolidine; DFT

1. Introduction

The fullerene derivatives are of interest for obtaining new biologically active compounds and materials for nanotechnology [1,2]. In the last few years, a considerable amount of attention has focused on biological properties of fullerenes and their derivatives after some promising studies, which demonstrated that there is inhibition of the HIV-P in the presence of C_{60} [3–5]. Also, there have been plenty of biological applications of C_{60} and evidence that some of its derivatives have been involved in DNA photocleavage [6], inhibition of apoptosis [7] and even act as a radical scavenger [8].

Biological applications of C_{60}–fullerene complexes are generally difficult because of its hydrophobic nonpolar nature, which causes them to have low solubility in water and polar solvents [9]. Fulleropyrrolidines are among the most studied fullerene derivatives, which have been used for numerous biological applications [10,11]. There are many polar and hydrophilic groups, which have introduced on the fulleropyrrolidine skeleton via substitution to the nitrogen or carbon atoms of pyrrodine moiety to improve its dissolvability as well as its biocompatibility profile [12–15].

In recent years, many trials have been carried out to substitute the fulleropyrrolidine with some commonly used drugs or biological compounds that have polar properties in order to investigate their biologically active nature. Thus, functionalized fullerenes may serve as novel systems for the delivery of drugs, antigens and genes into biological systems [6,13,16,17].

Organoselenium compounds have been described as promising pharmacological agents in view of their unique biological properties: chemopreventive, antioxidant, antibacterial, antiviral, antifungal, antiparasitic, antiinflammatory and antihistamine agents [18]. Selenocysteine and selenomethionine amino acids are of interest due to their existence in the active site of several selenoenzymes

* Corresponding authors. Tel.: +1 520 621 6761; fax: +1 520 621 8047 (A.F. Jalbout); tel.: +964 7801046701 (A. J. Hameed).
E-mail addresses: ajalbout@u.arizona.edu (A.F. Jalbout), alijamail2003@yahoo.com (A.J. Hameed).

0022-328X/$ - see front matter © 2006 Elsevier B.V. All rights reserved.
doi:10.1016/j.jorganchem.2006.10.068

[19–21]. These selenoenzymes such as glutathione peroxidase (GPx) and iodothyronine deiodinase (ID) play a vital role of protecting the cell by free radical scavenging [22]. Organoselenocyanate compounds have shown promising results in a variety of chemopreventative studies [23]. These compounds inhibit carcinogenesis in some organs using animal models and are effective in both the initiation and post-initiation phase [24]. Thus, functionalization of fullerenes with polar organoselenium compounds may gave rise to new fullerene-based systems, which have new chemical and biological properties.

Currently, we present results of molecular orbital theoretical calculations used to predict the structural and electronic properties of some fullerene-based systems containing biological organoselenium derivatives using Density Functional Theory (DFT) calculations [25]. The methods implemented in this work [26] are currently the method of choice for the study of such properties for many of biological molecules. These theoretical studies may provide information of a number of important physical and chemical properties of such molecules.

In this work, we have investigated theoretically a series of 1-(4, 5 and 6-selenenyl derivatives-3-formyl-phenyl) pyrrolidinofullerenes molecules C_{60}–C_2H_4N–[3-(CHO)C_6H_3SeX], where X = CN, $CH_2CH(NH_2)CO_2H$ and $CH_2CH_2CH(NH_2)CO_2H$.

2. Computational details

The calculations presented in this work were carried out by using the GAUSSIAN03 suite of programs [27]. The hybrid Becke 3-Lee–Yang–Parr (B3LYP) exchange-correlation functional was applied for DFT calculations [28–30]. The geometries of the compounds and the frequencies were evaluated with the B3LYP/3-21G* theory method. Due to computational limitations and the large size of the system, we were unable to perform higher level optimizations and frequencies on the systems. In addition, NMR constants were evaluated using the GIAO method [30]. In order to evaluate the thermodynamic stability of these molecules at elevated temperatures, we have applied the Shomate equations as recommended by the NIST database [31].

3. Results and discussion

3.1. Selenocyanate (SeCN) group

Fig. 1 displays the optimized B3LYP/3-21G* geometries of the selenocyanate (SeCN) group considered in this work. The figures shows bond lengths in angstroms (Å) and bond angles in degrees (°). In the figure, the yellow spheres are C atoms, blue spheres are H atoms, red spheres are N atoms, and orange spheres are Se atoms.

As we can see the structures for the *ortho* and *meta* structures are quite similar however, the *para* has a modified structure. The parameters shown in the figure are characteristic of such molecules, and as the figure shows the values are quite consistent between the different configurations. The most interesting aspect of the three molecules in the first category is the interaction between the Se atom and O of the COH group. The distances between the two structures are around 2.5 Å, which is relatively consistent with previous calculations of similar systems [25]. This distance is the average length needed for chalcogenide–metal (i.e. O–Se) interactions. The most profound geometrical difference is in the formation of the *para* structure. In this latter molecule the ring undergoes a drastic shift with relation to the five membered ring attached to the fullerene structure. The reason for this shift has to do partially with the fact that the Se atom now interacts with the N atom of the five membered ring. In the *para* structure, the interaction distance between the two atoms is around 2.72 Å.

In Table 1 we have shown the vibrational frequencies (cm^{-1}) for the three CN group structures. As one can see there is slight variation between the molecules, however, the largest difference has to do with the interaction of the Se with O of the COH group. This value is highest for the *ortho* structure, but lower for the *meta* and *para* molecules due to this effect. The frequency for this vibrational mode also affects the stretch mode of the CO group, which causes the *ortho* frequency to lower due to the fact that the Se interacts with the oxygen atom lowering the CO bond strength. The other vibrational frequencies are relatively similar. Interestingly, the vibrational frequency of the Se–N interaction (of the five membered ring attached the fullerene) is around 228 cm^{-1}, which is higher than the value of 194 cm^{-1} for Se–O interaction vibrational mode in the *ortho* structure.

In addition, to the theoretical vibrational IR spectrum the GIAO NMR computed shifts also show slight differences between the different isomers. If we consider the Se shifts of the *ortho* structure we obtain a value of around 1586 ppm compared to 1693 and 1686 for the *meta* and *para* structures, respectively. The lower value for the *ortho* molecule is probably due to the interaction of the Se atom with the CO group. The trends are similar for the other atoms in the molecule. The O (of the CO) group of the *ortho* species has a shift of around −238.9 ppm, *meta* has a value of −310.9 ppm and *para* has a value of around −308.5 ppm. Another interesting feature is that the N shift of the five membered ring exhibits slight differences between the three configurations. Chemical shifts (in ppm) of 197.7, 192 and 204 are observed for the *ortho*, *meta* and *para* isomers, respectively. The sudden shift in the *para* values are probably the result of the Se–N interactions due to their closer proximity (of 2.72 Å) in this structure.

Table 3 contains the physical properties of the various molecules considered in this study. As we can see the HOMO/LUMO gaps are presented for which the *meta* structure has the highest value of 1.976 eV, for which the *ortho* and *para* structures have lower values of 1.787 and 1.972 eV, respectively. The large gap for the *meta* isomer can probably be attributed to the reduced torsional potential

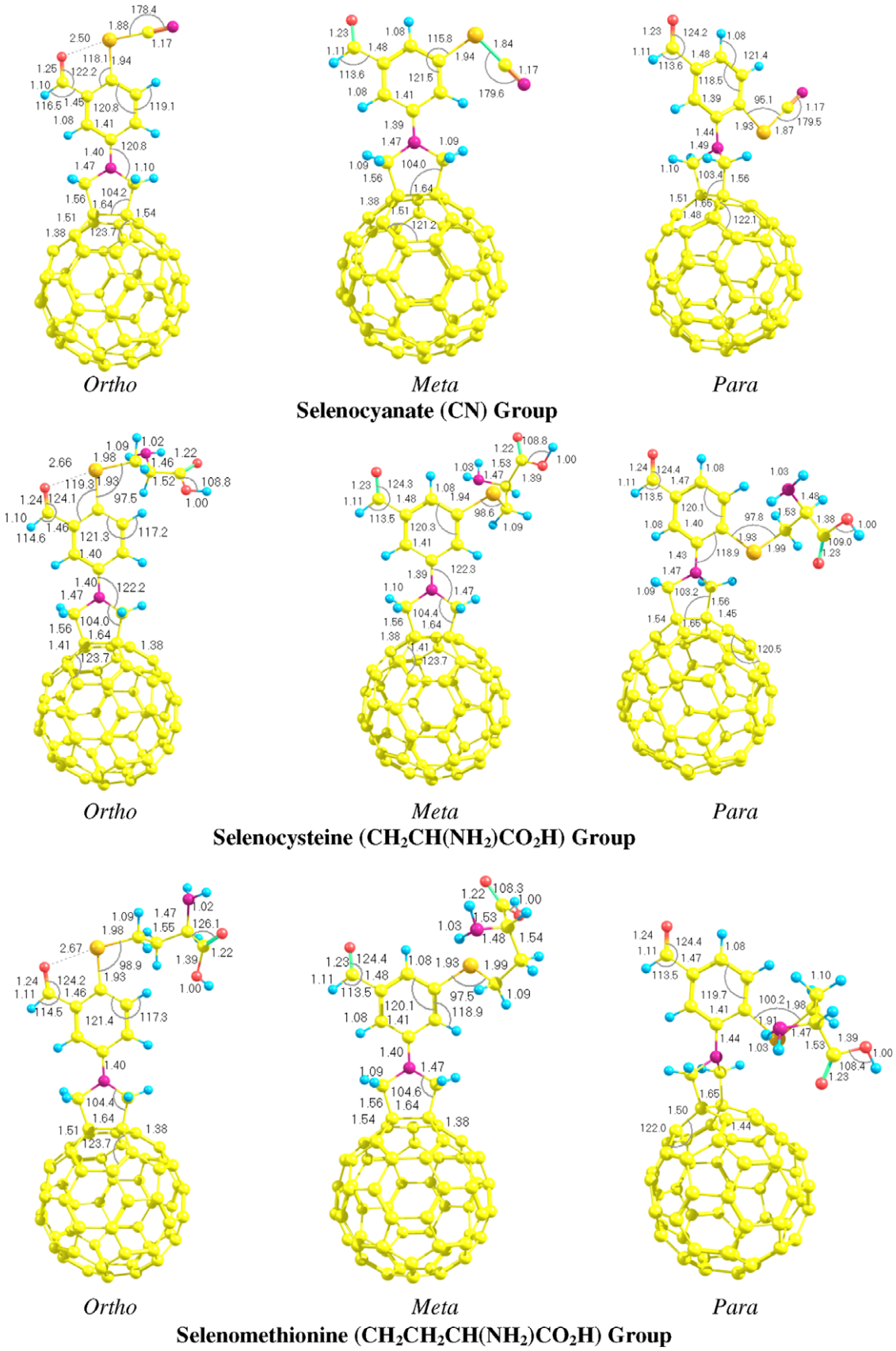

Fig. 1. Selected structural parameters with bond lengths shown in angstroms (Å) and bond angles in degrees (°) computed using the B3LYP/3-21G* method. In the figure, the yellow spheres are C atoms, blue spheres are H atoms, red spheres are N atoms, and orange spheres are Se atoms. (For interpretation of the references in color in this figure legend, the reader is referred to the web version of this article.)

Table 1
Vibrational analysis (frequencies are shown in cm^{-1}) for the isomers of the CN group with descriptions at the B3LYP/3-21G* level of theory

Vibrational mode	*ortho*	*meta*	*para*
SeCN wag	98	88	93
SeCN twist	462	465	450
Se–O (CO) stretch	194	163	120
CO group stretch	1646	1718	1716
Se–C (CN) stretch	503	481	485
CC stretch (five membered ring, carbon atoms directly attached to C_{60})	910	932	900
CH_2 rock (Five membered ring)	1005	1006	1002
C–H stretch (CO group)	3005	2925	2919
CH twist (phenyl ring)	1212	1217	1218
CH_2 twist (five membered ring)	1273	1276	1266
C–N stretch (phenyl-five membered ring connection)	1394	1383	1415
CH deformation (phenyl ring)	1465	1475	1459
CN group stretch	2247	2249	2252
CH stretch (five membered ring)	3126	3139	3143
CH stretch (phenyl ring)	3217	3213	3230

Table 2
Vibrational analysis (frequencies are shown in cm^{-1}) for the isomers of the $CH_2CH(NH_2)CO_2H$ group and the $CH_2CH_2CH(NH_2)CO_2H$ group with descriptions at the B3LYP/3-21G* level of theory

Vibrational mode	$CH_2CH(NH_2)CO_2H$ group			$CH_2CH_2CH(NH_2)CO_2H$ group		
	ortho	*meta*	*para*	*ortho*	*meta*	*para*
Se–O (CO) stretch	126	116	96	188	165	117
CO group stretch	1670	1718	1714	1671	1719	1712
NH_2–CH twist	1417	1399	1391	1333	1408	1405
NH_2 group stretch	1673	1718	1691	1683	1735	1737
NH stretch (NH_2 group)	3457	3371	3368	3440	3367	3375
NH_2 group twist	3571	3467	3482	3551	3464	3468
CO stretch ($CH_2CH(NH_2)CO_2H$ group)	1793	1782	1758	1783	1778	1772
COH twist (CO of CO_2H in the $CH_2CH(NH_2)CO_2H$ group)	1348	1312	1326	1359	1351	1331
C–H stretch (CO group in the $CH_2CH(NH_2)CO_2H$ group)	3482	3457	3472	3474	3460	3452
CC stretch (five membered ring, carbon atoms directly attached to C_{60})	903	907	900	908	1014	1002
CH_2 rock (five membered ring)	1018	1013	1028	1006	1026	1022
C–H stretch (CO group)	2946	2913	2909	2939	2911	2913
CH twist (phenyl ring)	1194	1126	1117	1118	1115	1126
CH_2 twist (five membered ring)	1272	1274	1266	1275	1270	1259
C–N stretch (phenyl-five membered ring connection)	1396	1393	1343	1381	1377	1338
CH deformation (phenyl ring)	1465	1464	1457	1463	1466	1459
CH stretch (five membered ring)	3133	3125	3169	3126	3124	3142
CH stretch (phenyl ring)	3209	3213	3192	3207	3226	3230

and interaction between the substituted groups. The lower values of the HOMO/LUMO gap for the *ortho* structure has to do with the fact that it has stronger interactions between the selenium and oxygen atom. The table also shows that the *ortho* structure is the lowest in energy (relative energies are denoted as $E_h^{3\text{-}21G^*}$, where 0 K are the relative energies including zero-point corrections) with the *meta* and *para* structures have a relative energy of 7.6 and 4.1 kcal/mol, respectively.

Table 4 shows the thermodynamic properties for the molecules in Fig. 1: entropy, heat capacity at constant pressure and enthalpy content at three different temperatures calculated using B3LYP/3-21G* frequencies. These fits were performed according to the equations implemented by the National Institute of Standards and Technology (NIST) [31]. For these calculations, the correct thermal energies shown in Table 3 (E^{corr}) are computed using the basic thermodynamic relationship, where the free energy changes are described as: $\Delta H - TS$, where ΔH is the enthalpy change, T is the temperature, and S is the entropy. In the table, E^{corr} (298.15 K) are the basic thermally corrected relative energies at room temperature and E^{corr} (1000 K) are the thermally corrected relative energies at an elevated temperature of 1000 K. As one can see the *meta* structure is around 0.6 kcal/mol higher in energy than the *ortho* structure at 298.15 K and 1.6 K higher at 1000 K. The difference in energy between *ortho* and *para* is also drastically reduced when thermal corrections are included as the value of 0.35 kcal/mol (at 298.15 K) and 0.2 kcal/mol (at 1000 K) are computed. Although, the values vary the general trend that is important to recognize is that the Se–O interaction in the *ortho* structure dominates the Se–N as in the *para* structure in terms of stability, since the distances between these atoms are similar in both con-

Table 3
Physical and chemical properties of the isomers

Physical property	CN			$CH_2CH(NH_2)CO_2H$			$CH_2CH_2CH(NH_2)CO_2H$		
	ortho	*meta*	*para*	*ortho*	*meta*	*para*	*ortho*	*meta*	*para*
HOMO/LUMO gap	1.787	1.976	1.972	1.237	1.831	1.911	1.560	1.734	1.926
B3LYP/3-21G*	−5231.3942322	−5231.3814075	−5231.3871877	−5460.4221652	−5460.4182741	−5460.4242381	−5499.5258774	−5499.5182031	−5499.5210511
B3LYP/3-21G* (0 K)	−5230.8615460	−5230.8495040	−5230.8550550	−5459.8007690	−5459.7970520	−5459.8023570	−5498.8751550	−5498.8673870	−5498.8707490
ZPE	0.532686	0.531903	0.532133	0.621397	0.621222	0.621882	0.650723	0.650816	0.650302
$E_h^{3\text{-}21G^*}$ [a] (kcal/mol)	0.000	8.047	4.420	1.301	3.742	0.000	0.000	4.816	3.029
$E_h^{3-21G^*}$ [a] (0 K) (kcal./mol)	0.000	7.556	4.073	0.996	3.329	0.000	0.000	4.874	2.765
H(298.15 K) − *H*(0) (kcal/mol)	94.15	95.39	94.49	108.57	106.11	107.32	110.94	111.42	110.96
H (1000 K) − *H*(0) (kcal/mol)	1033.41	1035.22	1034.06	1148.49	1139.98	1146.42	1177.84	1177.90	1178.02
S (298.15 K) (cal/mol K)	713.18	715.35	713.15	795.54	786.26	791.85	813.88	813.36	813.42
S (1000 K) (cal/mol K)	1693.02	1693.25	1693.47	1876.58	1868.28	1876.50	1929.10	1928.69	1929.47
E^{corr} [b] (298.15 K)	0.000	0.593	0.349	0.150	0.457	0.000	0.000	0.635	0.157
E^{corr} [b] (1000 K)	0.000	1.580	0.200	1.990	1.780	0.000	0.000	0.470	0.190

Total and relative energies were obtained at different levels of theory, while all other properties were calculated at the B3LYP/3-21G* level. Also, shown are the zero-point energies (ZPE) in hatrees/particle (E_h), where 0 K is the sum of electronic and zero-point energies.

[a] Relative B3LYP/6-31G* energies computed using B3LYP/3-21G* geometries and frequencies.

[b] E^{corr} are the corrected thermal energies (kcal/mol) at elevated temperatures, for which the fitted relationships are shown in Table 4.

Table 4
Thermodynamic properties of the molecule in Fig. 1, calculated using frequencies obtained at the B3LYP/3-21G* level, where C_p is the heat capacity in J mol^{-1} K^{-1}, S is the entropy in J mol^{-1} K^{-1}, and ΔH is the standard enthalpy kJ mol^{-1}

			Fitted thermodynamic equation ($T/1000 = t$)	100 K	298.15 K	1000 K
CN Group	*ortho*	C_p	$106.49522 + 2460.41858 * t + 210.15584 * t^2 - 426.16145 * t^3 + 0.86213 * t^{-2}$	439.96	854.14	2353.92
		S	$-330.34865 * \ln(t) + 6748.36481 * t - 11140.34859 * t^2/2 + 5306.1985 * t^3/3 + 0.7129/(2 * t^2) - 1253.5723$	163.60	713.18	1693.02
		ΔH	$-515.04907 * t + 5223.79391 * t^2/2 - 4395.78346 * t^3/3 + 1378.70369 * t^4/4 - 2.35649/t + 59.49738$	9.12	94.15	1033.41
	meta	C_p	$126.03804 + 2472.6367 * t + 194.97225 * t^2 - 419.80798 * t^3 + 0.8304 * t^{-2}$	457.41	875.81	2376.80
		S	$-333.15047 * \ln(t) + 6749.32732 * t - 11137.53479 * t^2/2 + 5304.87841 * t^3/3 + 0.72912/(2 * t^2) - 1255.27439$	169.27	715.35	1693.25
		ΔH	$-512.06074 * t + 5219.09295 * t^2/2 - 4395.46826 * t^3/3 + 1380.35832 * t^4/4 - 2.39988/t + 60.19610$	9.66	95.39	1035.22
	para	C_p	$111.37459 + 2455.80648 * t + 218.49779 * t^2 - 430.29527 * t^3 + 0.85169 * t^{-2}$	443.41	858.13	2358.40
		S	$-334.60394 * \ln(t) + 6784.41382 * t - 11211.57007 * t^2/2 + 5346.28731 * t^3/3 + 0.75970/(2 * t^2) - 1266.93186$	165.64	713.15	1693.47
		ΔH	$-519.38404 * t + 5241.96456 * t^2/2 - 4418.36432 * t^3/3 + 1387.8609 * t^4/4 - 2.41412/t + 60.69381$	9.39	94.49	1034.06
$CH_2CH(NH_2)CO_2H$ group	*ortho*	C_p	$141.37297 + 2766.17007 * t + 159.95503 * t^2 - 434.81962 * t^3 + 0.80316 * t^{-2}$	498.99	974.74	2635.72
		S	$-418.67027 * \ln(t) + 7596.43470 * t - 12431.27819 * t^2/2 + 5919.38066 * t^3/3 + 0.33062/(2 * t^2) - 1476.71801$	203.26	795.54	1876.58
		ΔH	$-538.62638 * t + 5653.7304 * t^2/2 - 4709.\ 66907 * t^3/3 + 1469.33194 * t^4/4 - 2.67292/t + 65.4706$	11.62	108.57	1148.49
	meta	C_p	$126.755100 + 2713.06327 * t + 209.7395 * t^2 - 453.77941 * t^3 + 0.83347 * t^{-2}$	482.56	948.48	2598.90
		S	$-426.07039 * \ln(t) + 7642.01128 * t - 12509.81519 * t^2/2 + 5961.29195 * t^3/3 + 0.30751/(2 * t^2) - 1505.26988$	194.77	786.26	1868.28
		ΔH	$-551.267200 * t + 5667.54417 * t^2/2 - 4725.43329 * t^3/3 + 1475.54462 * t^4/4 - 2.714700/t + 66.43874$	10.97	106.11	1139.98
	para	C_p	$131.27172 + 2739.32596 * t + 194.47619 * t^2 - 449.55327 * t^3 + 0.82701 * t^{-2}$	488.91	959.52	2618.63
		S	$-427.71174 * \ln(t) + 7670.52013 * t - 12563.22684 * t^2/2 + 5988.77283 * t^3/3 + 0.30344/(2 * t^2) - 1508.00901$	198.20	791.85	1876.50
		ΔH	$-549.99423 * t + 5687.73547 * t^2/2 - 4746.5692 * t^3/3 + 1483.59133 * t^4/4 - 2.71649/t + 66.54498$	11.28	107.32	1146.42
$CH_2CH_2CH(NH_2)CO_2H$ group	*ortho*	C_p	$136.68563 + 2821.11851 * t + 179.52127 * t^2 - 449.31251 * t^3 + 0.80964 * t^{-2}$	500.62	987.83	2691.10
		S	$-459.17385 * \ln(t) + 7904.8508 * t - 12867.81349 * t^2/2 + 6117.02645 * t^3/3 + 0.04588/(2 * t^2) - 1580.05767$	207.67	813.88	1929.10
		ΔH	$-549.30277 * t + 5764.9734 * t^2/2 - 4767.32788 * t^3/3 + 1478.69107 * t^4/4 - 2.74997/t + 66.83096$	11.68	110.94	1177.84
	meta	C_p	$151.36527 + 2814.99541 * t + 185.58176 * t^2 - 451.54385 * t^3 + 0.78939 * t^{-2}$	512.72	1000.93	2703.47
		S	$-467.58166 * \ln(t) + 7944.19932 * t - 12926.69088 * t^2/2 + 6146.23165 * t^3/3 + 0.04516/(2 * t^2) - 1600.10097$	210.60	813.36	1928.69
		ΔH	$211.63467 * t + 2119.21366 * t^2/2 + 974.3187 * t^3/3 - 1428.11132 * t^4/4 + 4.64934/t - 66.32502$	12.04	111.42	1177.90
	para	C_p	$134.76063 + 2815.96201 * t + 188.47264 * t^2 - 453.70797 * t^3 + 0.81534 * t^{-2}$	498.83	985.08	2688.60
		S	$-457.56641 * \ln(t) + 7914.99675 * t - 12900.72752 * t^2/2 + 6138.78363 * t^3/3 + 0.10658/(2 * t^2) - 1580.64787$	207.27	813.42	1929.47
		ΔH	$-552.60303 * t + 5778.13105 * t^2/2 - 4782.\ 14693 * t^3/3 + 1483.89327 * t^4/4 - 2.76124/t + 67.38266$	11.85	110.96	1178.02

These where fitted to the Shomate equations, which are implemented by the JANAF tables of the NIST databases.

figurations (2.5 Å between Se–O and 2.7 Å between Se–N). This stabilization energy roughly corresponds to around 4.1 kcal/mol.

3.2. Selenocysteine ($SeCH_2CH(NH_2)CO_2H$) group

In the second $SeCH_2CH(NH_2)CO_2H$ group we observe some very similar trends as we have seen for the SeCN group in the last section. As we can see the *ortho* structure again, exhibits relative interaction between the Se and O of the CO group. The interaction distance between the Se–O is around 2.66 Å which is slightly larger than the previous case, probably due to the presence of a larger $CH_2CH(NH_2)CO_2H$ group attached to the Se atom. All other geometrical parameters are very consistent between the through structural orientations. However, as in the previous case the *para* structure undergoes a rotation of the five membered ring to allow for stronger Se–N (of the five membered ring) interactions to take place.

The vibrational mode analysis for these sets of molecules are shown in Table 2. As we can see the Se–O stretch is higher for the *ortho* molecule relative to the *meta* and *para* structures due to the strong selenium chalcognide interactions. The remainder of the frequencies are typical and do not vary much between the *ortho*, *meta* and *para* orientations. Interestingly, as we will discuss shortly, the *para* structure is the lowest energy structure. This can be attributed to the fact the Se–N (of the five membered ring) interaction occurs at a distance of about 3 Å with a vibrational mode corresponding to 243 cm^{-1}. Also, the C–N distance (between the carbon atom of the phenyl ring and the nitrogen atom of the five membered ring) is lower for the *para* structure, which can allude to the fact that electron density of the nitrogen is slightly distorted by the presence of the selenium atom. The GIAO NMR shifts aids to substantiate this conclusion as well. The Se shifts for the *ortho*, *meta* and *para* structures are 1590.4, 1664.0 and 1741.8 ppm, respectively. Also, the N shifts of the five membered ring are 144.6, 196.3 and 204.8 ppm for *ortho*, *meta*, and *para*, respectively. We obtain shifts of the oxygen atom (of the CO group) corresponding to −238.9, −310.9, and −308.5 ppm for *ortho*, *meta* and *para*, respectively. These trends reinforce the trend that the Se–O interactions cause significant differences in the shifts between the three configurations. In addition, the fact the N shift is higher for *para* also helps to reiterate the fact that the Se–N interactions can lead to a stabilization effect in that structure. In this case the Se–N interaction dominates the Se–O interaction causing the *para* structure to be lower in energy than the *ortho* structure.

Table 3 presents physical properties for this group as well. The table also shows that the *ortho* structure has a lower HOMO/LUMO gap than the *meta* and *para* structure as was observed for the CN group. The interesting feature of this system is that the *para* structure is lower in energy than the other systems. The relative energies of the *ortho* and *meta* systems (with zero-point effects factored in) are about 1.0 kcal/mol and 3.3 kcal/mol, respectively. Another interesting point, is that when thermal corrections are added the *ortho* structure is higher in energy than the *meta* structure at elevated temperature. This can be due to the fact that at increased temperatures the Se–O interaction is weakened due to rotational effects of the internal bonds in the molecule. The decreased overall stability of the *ortho* structure may be due to the fact that the $SeCH_2CH(NH_2)CO_2H$ group is relatively bulky and causes too much internal congestion in this orientation. While the steric effects may cause slight destabilization, the Se–O interaction causes the molecule to have lower energy than the *meta* structure where no internal interactions are predominantly evident.

3.3. Selenomethionine ($SeCH_2CH_2CH(NH_2)CO_2H$) group

In the last group $SeCH_2CH_2CH(NH_2)CO_2H$ there are minor differences to the formerly discussed set of molecules. This molecular group is almost identical to the selenocysteine molecular set, except for the fact that the NH_2 group changes position along the carbon chain attached to the Se atom. As we can see from Fig. 1, the relative differences in the structures are small, with again the *para* structure forming a strong Se–N interaction with the five membered ring attached to the fullerene. The computed frequency analysis for these sets of molecules are also shown in Table 2. Again, as Table 2 shows the relative vibrational frequencies are almost the same. The major differences, are attributed to the Se–O (of the CO group) frequency as well as the C–N stretch (between the carbon atom of the phenyl ring and the nitrogen atom of the five membered ring). In the former case, the *ortho* has a higher value than the other structures due to the stronger Se–O interaction and as in the previous system the C–N frequency is lowered in the *para* case due to the Se–N interaction.

If we analyze the GIAO NMR chemical shifts we can observe the same situation as in the previous case. In this case we obtain an N shift (of the five membered ring) of 201.9, 197.6, 209.4 ppm for *ortho*, *meta*, and *para* respectively. We compute Se shifts of 1591.2 (*ortho*), 1727.3 (*meta*), and 1697.1 (*para*) ppm for and O (of the CO group) shifts of −270.6 (*ortho*), −311.5 (*meta*), −297.4 (*para*) ppm. Again, the increased Se–O interactions cause changes in their representative shifts, and the Se–N of the*para* structure cause significant N shifts as well.

From Table 3 we can see that the HOMO/LUMO gaps are very similar to the previously investigated system, whereby the *ortho* structure has the lowest value, *meta* the next highest, and *para* has the largest value. However, in this system, the *ortho* structure again is lower in energy than the *meta* and *para* molecules. In this molecule, the fact that the NH_2 group is placed further away from the Se atom causes the *ortho* structure to have less steric hindrance upon the Se–O interaction junction point. This causes it to have a lower energy than the *para* structure

and the *meta* structure. In the *para* structure, while there is a relatively strong Se–N interaction that occurs at a distance of 2.8 Å with a corresponding vibrational frequency of 236 cm^{-1}, the NH_2 group rotates in such a way that causes slight destabilization effects via interaction with the Se atom. Table 3 shows that the *meta* structure is around 4.9 kcal/mol higher than the *ortho* molecule, and that the *para* structure is around 2.8 kcal/mol higher. With thermal corrections included the table shows the values are significantly reduced, however, *para* still remains lower in energy than *meta*. This means the Se–N interaction in the *para* structure is relatively strong at normal and elevated temperatures.

4. Conclusions

In this work we have studied the theoretical structure, IR spectra, NMR and energetics of the *ortho*, *meta* and *para* forms of 1-(4, 5 and 6-selenenyl derivatives-3-formyl-phenyl) pyrrolidinofullerene derivatives at the B3LYP/3-21G* level of theory. We have seen that selenocyanide systems conserve the general trend that the *ortho* structure is more stable than the *meta* and *para* structures. The same is true for the selenomethionine ($SeCH_2CH_2CH(NH_2)CO_2H$) group, however in the selenocysteine ($SeCH_2CH(NH_2)CO_2H$) group the *para* structure is in fact the lowest energy structure. As we have discussed in this paper, the reason has to do with the fact the *ortho* structure has stabilization effects due to the fact that the Se–O interactions are relatively strong causing the molecule to be lower in energy. Alternatively, the *para* structure has the characteristic that the molecules undergo drastic rotations causing the Se and N (of the five membered ring attached to the fullerene molecule) to interact. In the selenocysteine system, however, the close proximity of the NH_2 group to the Se–O interaction point causes steric effects to slightly reduce the energy of the system, which permits the *para* structure to assume a lower energy.

In relation to our previous calculations [25] we have shown that Se has the ability to positively mediate charge in a molecular species, which may serve a useful role in many biochemical mechanisms. Molecular stabilization of free radicals (i.e. by being trapped by the Se atom or by occupying electronic density around the Se–O interaction junction) can allow for a positive prevention of many potentially harmful conditions, such as cancer, or DNA mutations [32]. Due to the fact that Se can mediate charge (since these molecules have negative LUMO energies, which tells us that there is a propensity towards electron attachment), the anion forms of such molecules can prevent DNA damaging effects of radiation and free radicals in the body. Also, the fact that we have explored systems with polar groups, it may provide insight into a new type of water soluble system that is effective in molecular entrapment of free radicals in a biological system.

Our work can be useful for experimentalists to pursue the electronic structure of this molecule further. This work extends our investigations into potentially important water soluble fullerene systems that can be stabilized by chalcogenide–selenium interactions and can be proposed as potential electron traps as well. We believe that these systems are realistically feasible structures that deserve further attention. Due to the large size of the molecules explored we were unable to perform higher level *ab initio* computations due to the lack of computational resources. However, in the computation of physical properties and vibrational frequencies DFT has been shown to be in good agreement to MP2 and related computational approaches [33].

Acknowledgements

A.J. Hameed would like to thank Dr. Najeh Al-Salim (NZ Crown Research Institute for Industrial Research, New Zealand) and A.F. Jalbout appreciates the NASA Astrobiology Institute (USA) and the National Autonomous University of Mexico for generous support. Supplementary materials with the *xyz* coordinates of all structures and the thermochemistry data are also available.

References

[1] N.R. Scott, Rev. Sci. Tech. Oie. 24 (2005) 425.
[2] N. Martín, Chem. Commun. (2006) 2093.
[3] S.H. Friedman, D.L. DeCamp, R.P. Sijbesma, G. Srdanov, F. Wudl, G.L. Kenyon, J. Am. Chem. Soc. 115 (1993) 6506.
[4] S.H. Friedman, P.S. Ganapathi, Y. Rubin, G.L. Kenyon, J. Med. Chem. 41 (1998) 2424.
[5] R. Sijbesma, G. Srdanov, F. Wudl, J.A. Castoro, C. Wilkins, S.H. Friedman, D.L. DeCamp, G.L. Kenyon, J. Am. Chem. Soc. 115 (1993) 6510.
[6] T. Da Ros, E. Vázquez, G. Spalluto, S. Moro, A. Boutorine, M. Prato, J. Supramol. Chem. 2 (2002) 327.
[7] M. Bisaglia, B. Natalini, R. Pellicciari, E. Straface, W. Malorni, D. Monti, C. Franceschi, G.J. Schettini, Neurochemistry 74 (2000) 1179.
[8] L.L. Dugan, D.M. Turetsky, C. Du, D. Lobner, M. Wheeler, C.R. Almli, C.K.-F. Shen, T.-Y. Luh, D.W. Choi, T.-S. Lin, Proc. Natl. Acad. Sci. U.S.A. 94 (1997) 9434.
[9] R.S. Ruoff, D.S. Tse, R. Malhotra, D.C. Lorents, J. Phys. Chem. 97 (1993) 379.
[10] M. Prato, M. Maggini, Acc. Chem. Res. 31 (1998) 19.
[11] N. Tagmatarchis, M. Prato, Synlett (2003) 768.
[12] T. Da Ros, G. Spalluto, M. Prato, CCACAA 74 (2001) 743.
[13] B.M. Illescas, R. Martínez-Alvarez, J. Fernández-Gadeab, N. Martín, Tetrahedron 59 (2003) 6569.
[14] P. Brough, C. Klumpp, A. Bianco, S. Campidelli, M. Prato, J. Org. Chem. 71 (2006) 2014.
[15] A. Mateo-Alonso, C. Sooambar, M. Prato, Org. Biomol. Chem. 4 (2006) 1629.
[16] A. Bianco, K. Kostarelos, C.D. Partidos, M. Prato, Chem. Commun. (2005) 571.
[17] P. De Maria, A. Fontana, C. Gasbarri, D. Velluto, Soft. Matter 2 (2006) 595.
[18] (a) R.F. Burk, Selenium in Biology and Human Health, Springer-Verlag, New York, 1994;
(b) D.L. Hatfield, Selenium. Its Molecular Biology and Role in human Health, Kluwer Academic Publishers, Boston, 2001.
[19] J.C. Davey, K.B. Becker, M.J. Schneider, D.L. St. Germain, V.A. Gaton, J. Biol. Chem. 270 (1995) 26786.
[20] W. Croteau, S.L. Whittemore, M.J. Schneider, D.L. St. Germain, J. Biol. Chem. 270 (1995) 16569.

[21] R.P. Larsen, M.J. Berry, Ann. Rev. Nutr. 15 (1995) 323.
[22] (a) T.C. Stadtman, Annu. Rev. Biochem. 65 (1996) 83;
(b) Y. Saito, K. Takahashi, J. Health Sci. 46 (2000) 409.
[23] S. Sugie, T. Tanaka, K. El-Bayoumy, J. Health Sci. 46 (2000) 422.
[24] R. Sinha, K. El-Bayoumy, Curr. Cancer Drug Targets 4 (2004) 13.
[25] A.F. Jalbout, B. Trzaskowski, A.J. Hameed, J. Organomet. Chem. 691 (2006) 4589;
A.J. Hameed, A.F. Jalbout, B. Trzaskowksi, Int. J. Quantum. Chem. 107 (2007) 152.
[26] W. Koch, M.C. Holthausen, A Chemist's Guide to Density Functional Theory, Wiley-VCH Verlag GmbH, New York, 2001.
[27] M.J. Frisch et al., GAUSSIAN03, Revision B.05, Gaussian Inc., 2003.
[28] C. Lee, W. Yang, R.G. Parr, Phys. Rev. B 37 (1988) 785.
[29] A.D. Becke, J. Chem. Phys. 98 (1993) 5648.
[30] T. A Keith, R.F.W. Bader, Chem. Phys. Lett. 194 (1992) 1.
[31] P.J. Linstrom, W.G. Mallard (Eds.), NIST Chemistry WebBook, NIST Standard Reference Database Number 69, July 2001, National Institute of Standards and Technology, Gaithersburg MD, 20899. http://webbook.nist.gov.
[32] A.F. Jalbout, L. Adamowicz, Adv. Quant. Chem. 56 (2006) 1.
[33] A.F. Jalbout, F. Nazara, L. Turker, J. Mol. Struct. (THEOCHEM) 627 (2004) 1.